Supplementary material

MRI quality control

To ensure the consistent performance of MRI systems at the authors' institution a range of MRI parameters that are essential for accurate imaging and diagnosis are periodically evaluated using the ACR phantom (1,2).

This ACR phantom provides a standardized method for assessing the performance of different MRI systems across time points. This consistency is crucial for ensuring that imaging results are reliable and comparable, regardless of where or when the scans are performed. In particular, a more detailed breakdown of the specific tests that are performed is here reported:

1. Geometric Accuracy to ensures that the MRI system accurately represents the size and shape of objects, with absence of geometric distortion.
2. Slice Position Accuracy to verify that the MRI system is correctly positioning and orienting image slices.
3. Slice Thickness Accuracy to confirm that the MRI system is producing slices with the correct thickness.
4. Image Uniformity to ensure that the signal intensity is uniform across the entire image.
5. Contrast Resolution to assess the MRI system's ability to distinguish between tissues of slightly different signal intensities.
6. Spatial Resolution to evaluate the MRI system's ability to resolve small details within the image.
7. Image Artifact Evaluation to Identify any unwanted artifacts in the MRI images that could obscure important diagnostic information.

References

1. ELSE Solutions s.r.l: ACR MRI Phantom. https://www.elsesolutions.com/en/prodotti/radiodiagnostica/fantocci-risonanza/acr-mri-phantom/. Accessed August 1, 2024.
2. Palesi F, Nigri A, Gianeri R, Aquino D, Redolfi A, Biagi L, Carne I, De Francesco S, Ferraro S, Martucci P, *et al*: MRI data quality assessment for the RIN-Neuroimaging Network using the ACR phantoms. Phys Med 104: 93-100, 2022.

Figure S1. Correlation between duration of FTM therapy and volume difference (Pearson's correlation coefficient *r*=-0.169, P=0.516). FTM, fotemustine.

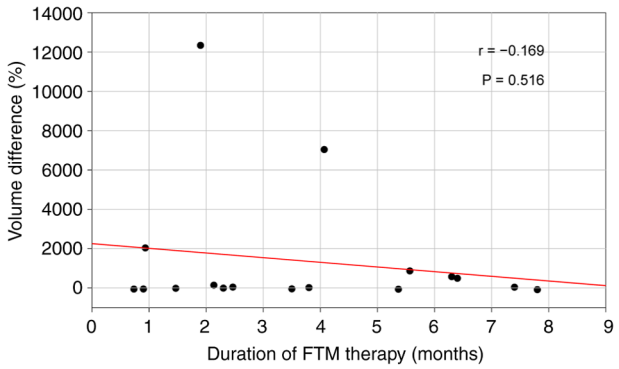

Figure S2. Correlation between duration of FTM therapy and ADC^{10} difference (Pearson's correlation coefficient *r*=-0.139, P=0.570). Of note, the non-significant correlation was confirmed also by using Spearman's correlation analysis (P=0.299) to account for the presence of outliers and by Pearson correlation analysis with exclusion of the outlier (P=0.180). FTM, fotemustine; ADC^{10}, tenth percentile of apparent diffusion coefficient.

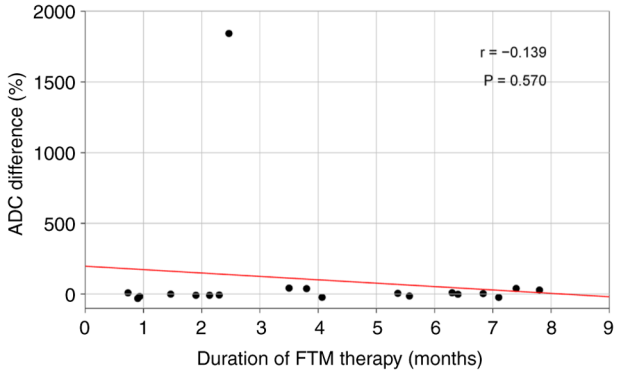

Figure S3. Correlation between survival after FTM start and volume difference (Pearson's correlation coefficient *r*=-0.199, P=0.444). Of note, the non-significant correlation was confirmed also by using Spearman's correlation analysis (P=0.293) to account for the presence of outliers and by Pearson correlation analysis with exclusion of the outlier (P=0.842). FTM, fotemustine.

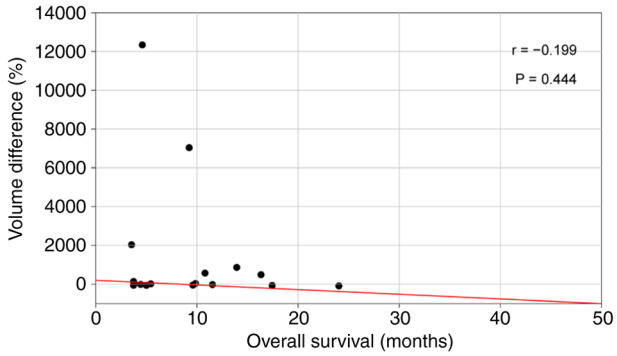

Figure S4. Correlation between survival after FTM start and ADC^{10} difference (Pearson's correlation coefficient *r*=-0.183, P=0.453). Of note, the non-significant correlation was confirmed also by using Spearman's correlation analysis (P=0.576) to account for the presence of outliers and by Pearson correlation analysis with exclusion of the outlier (P=0.723). FTM, fotemustine; ADC^{10}, tenth percentile of apparent diffusion coefficient.

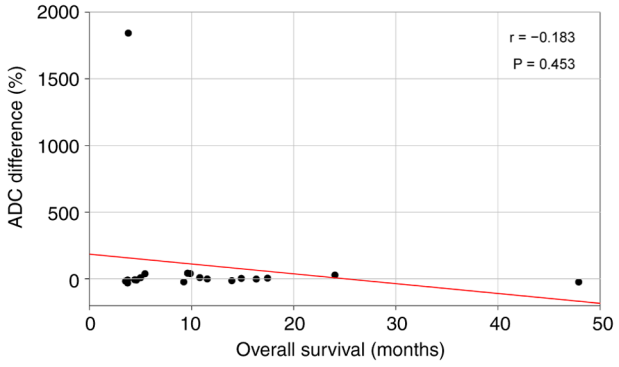

Figure S5. Survival curves stratified by MGMTp methylation status (P=0.89, log-rank test). MGMTp, O^6-methylguanine-DNA methyltransferase promoter.

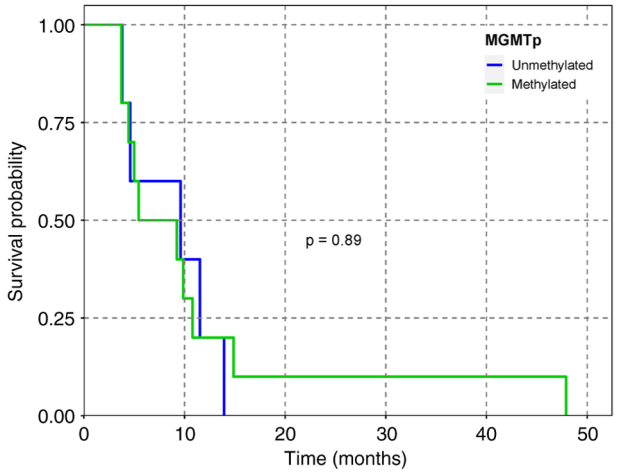

Figure S6. Survival curves stratified by IDH mutation (P=0.84, log-rank test). IDH, isocitrate dehydrogenase.

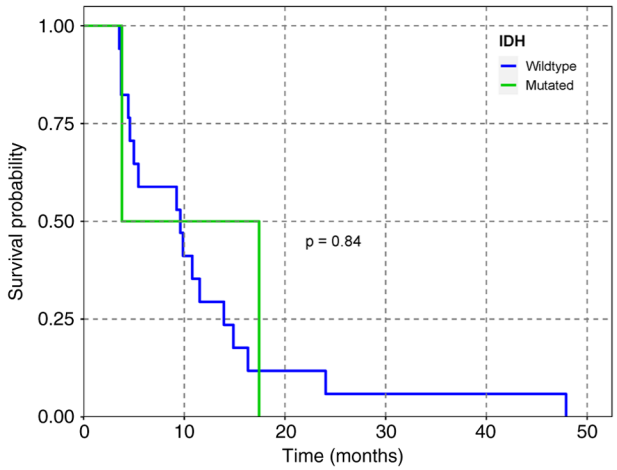

Figure S7. Correlation between duration of FTM therapy and survival after FTM start (Pearson's correlation coefficient r=0.669, P=0.002). FTM, fotemustine.